



NIH Public Access

Author Manuscript

Biomacromolecules. Author manuscript; available in PMC 2010 August 10.

Published in final edited form as:

Biomacromolecules. 2009 August 10; 10(8): 2019–2032. doi:10.1021/bm8012764.

Microfabricated electrospun collagen membranes for 3-D cancer models and drug screening applications

Olga Hartman^{1,a}, Chu Zhang^{2,6,a}, Elizabeth L. Adams^{3,2}, Mary C. Farach-Carson^{1,2,6}, Nicholas J. Petrelli⁴, Bruce D. Chase⁵, and John F. Rabolt^{1,*}

¹ Department of Materials Science and Engineering

² Department of Biological Sciences, University of Delaware

³ Delaware Biotechnology Institute

⁴ Helen F. Graham Cancer Center, Christina Care Health System

⁵ DuPont Central Research and Development

⁶ Center for Translational Cancer Research

Abstract

Invasive epithelial tumors form from cells that are released from their natural basement membrane and form 3-D structures that interact with each other and with the microenvironment of the stromal tissues around the tumor, which often contains collagen. Cancer cells, growing as monolayers on tissue culture plastic, do not reflect many of the properties of whole tumors. This shortcoming limits their ability to serve as models for testing of pharmacologically active compounds, including those that are being tested as anti-neoplastics. This work seeks to create new 3-D cellular materials possessing properties similar to those in native tissues surrounding cancers, specifically electrospun micro- and nanofibrous collagen scaffolds that support tumor growth in 3-D. We hypothesize that a 3-D culture system will provide a better replica of tumor growth in a native environment, and thus better report the bioactivity of anti-neoplastic agents. In addition, we optimized conditions, and identified physical characteristics that support growth of the highly invasive, prostate cancer bone metastatic cell line C4-2B on these matrices for use in anti-cancer drug studies. The effects of matrix porosity, fiber diameter, elasticity and surface roughness on growth of cancer cells were evaluated. Data indicates that while cells attach and grow well on both nano- and nanofibrous electrospun membranes, the nanofibrous membrane represented a better approximation of the tumor microenvironment. It was also observed that C4-2B non-adherent cells migrated through the depth of two electrospun membranes and formed colonies resembling tumors on day 3. An apoptosis study revealed that cells on electrospun substrates were more resistant to both anti-neoplastic agents, docetaxel (DOC) and camptothecin (CAM), compared to the cells grown on standard collagen-coated tissue culture polystyrene (TCP). Growth, survival, and apoptosis were measured, as well as the differences in the apoptotic capabilities of the two above mentioned compounds compared to known clinical performance. We conclude that 3-D electrospun membranes are amenable to high throughput screening for cancer cell susceptibility and combination killing

*Corresponding author. Address: Room 201 Dupont Hall, Department of Materials Science and Engineering, University of Delaware, Newark, DE 19716. Phone: (302) 831-4476. Fax: (302) 831-4545. rabolt@udel.edu.

¹ Author. Address: 15 Innovation Way, Room 244, Delaware Biotechnology Institute, University of Delaware, Newark, DE 19711. Phone: (302) 831-3454, Fax: (302) 831-4841. ohartman@udel.edu

^aThese authors contributed equally to this work

1. Introduction

The development of novel cell culture systems is vital for the improved yield and quality of high throughput compound screening, cell-based assays and *ex-vivo* drug testing. Three-dimensional fibrous collagen matrices that resemble native tissue architecture are of particular interest as they offer spatially open culture models which can be used to study cell phenotype in relation to matrix organization.² Most research efforts have focused on the growth of cells on collagen coated two-dimensional (2-D) matrices, such as flat tissue culture plates. However, major limitations when using flat 2-D plates are poor cell viability and changes in cell phenotype in response to the material surface.^{3–5}

Most existing methods of growing cells in 3-D microenvironments are unable to reproduce proper tissue microstructure and function.^{6–8} A better understanding of how microenvironment can influence cell signaling is required to create physiologically mimetic model systems, in which both normal and pathological cell and tissue functions can be studied.^{9,10} In cancer research, it is increasingly recognized that *in vitro* 3-D tissue culture models for drug screening are superior to a conventional monolayer of cells (2-D) grown on collagen-coated tissue culture polystyrene (TCP).^{11,12}

When designing a model culture system for prostate cancer cells, it is desirable to reconstruct the characteristic 3-D architecture of the native tissue in order to successfully investigate the pathobiology of the disease.¹¹ Cancer cells used in this study originate from epithelial cells, but then undergo epithelial-mesenchymal transition (EMT): they de-differentiate, break through the original basement membrane (BM), invade blood vessels, and migrate into bone marrow, where they assimilate in a new microenvironment, adopting a mesenchymal phenotype.¹³ Matrigel® may serve to mimic epithelial basement membrane tissues, providing dense (in term of small pore size) though less stiff media compared to bone microenvironment, where collagen type IV is a major component.¹⁴ For this study, collagen type I was chosen as the matrix material because it is a major component of stromal ECM found in bone.¹⁵ Microfabricated porous structures, described in this work, were designed to closely mimic the tumor microenvironment with randomly oriented, “loose” fibrous meshes that are structurally similar to extracellular matrix (ECM) found in bone.¹⁶

An important feature of metastatic cancer cells is their multicellular aggregation that correlates with high survival rate *in vitro*¹⁷ and increased metastatic potential *in vivo*.¹⁸ Multicellular aggregates form spheroids consisting of mixed cells (tumor and stromal) organized in 3-D structures. Such an arrangement induces cell-cell and cell-matrix interactions, affects penetration of drugs, and controls the accessibility and function of various adhesion molecules and growth factors. These biological factors provide important cellular signaling that contributes to the development of drug-resistant and highly invasive phenotypes by defining the regulatory mechanisms of cell growth, differentiation and death.¹⁹

The combination of microfabrication techniques with novel biomaterials provides a unique approach to generate artificial extracellular matrices that mimic native tissue microstructure. However, few studies have considered which material properties influence cell growth in 3-D environment. In this paper, we describe the design and characterization of electrospun fibrous collagen matrices used to culture C4-2B prostate cancer cells *in vitro*. This cell line, while one of the best cellular models for osteoblastic prostate cancer bone metastasis (derived from primary mouse bone marrow tumor cells), has proven to be less than ideal for drug testing, owing to its tendency to detach from plastic surfaces.²⁰ Our ability to overcome this obstacle by using electrospun membranes opens the door for use of this cell line in multi-well testing applications.

A variety of techniques for fabricating porous three-dimensional scaffolds including phase separation,^{21–23} electrospinning,²⁴ and self-assembly²⁵ have been developed. Among them, electrospinning provides a direct way to fabricate 3-D fibrous materials with properties similar to those found in native tumors. Electrospinning creates fibers in the form of non-woven mats on which cells are grown for characterization and testing of anti-cancer compounds. The fibers produced during the electrospinning process have micron to sub-micron diameters ranging from 100–5000 nm. One major advantage of electrospinning is that it uses very small quantities of starting material (5–100 mg, the quantity that might result from a custom synthesis). A second advantage is that additional components, e.g., small molecules, a second polymer, or cell binding factors can be added to the polymer solution and then incorporated into the fiber during electrospinning.

In our preliminary study (data not shown) we prepared a variety of electrospun collagen membranes that differed in porosity, fiber diameter, morphology, and extent of cross-linking in order to identify the optimum conditions for successful attachment and growth of cancer cells.^{26, 27} Two of these collagen membranes with superior cell attachment properties were selected for the current research. The goal of this work is to correlate physical properties of 3-D electrospun collagen scaffolds with their biological performance. Physical properties that have been investigated include: membrane geometry, its elastic modulus, membrane thickness, and its surface roughness. Biological performance investigated in this work relates to growth properties of cancer cells and their response to anti-cancer drugs when grown in a 3-D electrospun matrix. Though C4-2B cells represent the best cell line model to study highly invasive bone metastatic prostate cancer, its use in clinical research is highly limited. Non-adherent cells have rarely been investigated in the tissue engineering (TE) research as well, since they are more specific to metastatic cancer cell lines. These cells do not adhere well to the substrate so growing them on engineered substrates can be particularly challenging. Handling and manipulation of non-adherent cells during drug treatment is a major challenge for high throughput compounds screening, which puts significant limitations on the choice of cell lines for clinical research.

CAM is an anti-neoplastic drug that prevents DNA replication by inhibiting topoisomerase I. CAM and its derivatives are rapidly establishing themselves as a most promising group of new anti-neoplastic agents. Compared to other drugs at similar stages of development (phase III clinical trials) CAM has demonstrated a much higher anti-cancer activity, and it is envisioned as the ultimate anti-cancer drug when fully developed.²⁸ DOC, the most commonly prescribed drug for advanced prostate cancer, targets actin filaments in the cytoskeleton. On the basis of two recent phase III clinical trials, a regimen of docetaxel plus prednisone every 3 weeks is now considered standard first-line therapy for metastatic hormone-refractory prostate cancer disease.²⁹

Additionally, in this work as a part of biological characterization, we investigated: 1) the ability of metastatic prostate cancer cells to proliferate and migrate on various matrices; 2) apoptosis and drug resistance in 2-D and 3-D cultures; and 3) the relative efficacy of two anti-cancer drugs commonly used in clinical studies.

The significant extension of this research will be the development of a high throughput screening 3-D cell culture system, using electrospun collagen non-woven fibrous mats, in which cancer cell growth can be investigated. This approach will allow qualitative and quantitative assessment of growth, apoptosis and cell invasion, providing a sensitive and timely tool for testing of novel anti-neoplastic therapeutics.^{5, 11}

2. Materials and Methods

2.1. Materials

The first electrospun membrane (M1) was prepared using collagen type I from calf skin (Elastin Products Company, Owensville, MO) dissolved in a 1,1,1,3,3-hexafluoro-2-propanol (HFIP) (Sigma Aldrich, St. Louis, MO) solution at 16% (w/v) concentration. A second electrospun membrane (M2) was prepared from a solution of collagen in 2,2,2-trifluoroethanol (TFE) (Fisher Scientific, Pittsburgh, PA) at 16% (w/v) concentration. The calf skin collagen employed for the electrospinning of both membranes was used as received without further purification. Collagen-coated 96-well TCP plates were prepared by dissolving collagen type I (calf skin) in PBS buffer (Sigma-Aldrich, St. Louis, MO) at 15 µg/ml (w/v) and applying 50 µl of this solution to each well for 30 min followed by subsequent wash steps with PBS.

2.2. Electrospinning

Processing of collagen solutions into fibrous membranes by electrospinning was performed according to a procedure described elsewhere^{26, 30} where an electrospinning apparatus was employed to produce continuous fibers without beads. The 16% (w/v) collagen solutions in HFIP and TFE respectively were individually placed in a 3 mL syringe with attached needle (Hamilton, Columbus, OH) having a 0.51 mm inner diameter. A voltage of +15 kV (Glassman Series EH, Whitehouse Station, NJ) was applied to the tip of the needle. The grounded target, consisting of a 3' × 3' metal sheet covered in non-stick aluminum foil, was placed at a working distance (distance from the tip of a needle) of 13 cm. A flow rate of 2 ml/hr was applied via the syringe pump (KDS100, KD Scientific, Holliston, MA).

2.3. Crosslinking

Collagen fibers can be easily dissolved in aqueous media. Thus, the fibrous membranes must be cross-linked before any cellular work can be undertaken. The extent of cross-linking is a very important parameter for 3-D scaffold design because it, along with the spinning conditions, defines porosity, interconnectivity of the network, pore size, and pore size distribution. Glutaraldehyde (Sigma-Aldrich, St. Louis, MO), a commonly used cross-linking agent, was utilized to stabilize collagen fibers via a reaction between the carboxyl groups on the glutaraldehyde and the amide groups of the collagen, thus forming cross-links between polymer chains. Scheme 1 illustrates the proposed cross-linking reaction.³¹ Glutaraldehyde was used at 0.5 v/v (%) concentration for 21 h, vapor protocol,²⁹ to cross-link the collagen membranes. However, glutaraldehyde can be cytotoxic. In order to eliminate this negative effect, the membranes were incubated with 1% (w/v) glycine (Sigma Aldrich, St. Louis, MO) in PBS solution (Sigma, St. Louis, MO) to quench residual carboxyl groups and reduce the cytotoxicity. The collagen coating on the bottom of TCP plates was found to be less soluble and does not require additional fixation. Consequently, glycine treatment was not necessary.

2.4. Characterization of electrospun collagen membranes

2.4.1. Scanning Electron Microscopy—Electrospun collagen membranes were analyzed by Field Emission Scanning Electron Microscopy (FESEM, JSM 7400F, Jeol, Japan). Before FESEM imaging, the samples were coated directly with gold using a sputter coater (Jeol JFC-1200 fine coater, Japan). The diameters of many fibers were measured using NIH Image J Software. The average, mean and standard deviation are reported. To ensure accuracy of data, measurements were taken randomly at 30 different locations over the electrospun mat.

2.4.2. Atomic Force Microscopy—Fiber surface topographies were characterized with an Atomic Force Microscopy (AFM) (Nanoscope III, Veeco, Santa Barbara, CA) under ambient conditions in tapping mode using phosphorus doped silicon cantilevers (Veeco, Santa Barbara,

CA). The scan size used in the present study was $10\text{ }\mu\text{m} \times 10\text{ }\mu\text{m}$ in the X and Y directions. A roughness parameter for the surface R_q , (the root-mean-square height of the surface) was calculated using AFM software. The roughness data was acquired by manually applying a rectangular region of interest (ROI) box to different areas of the fiber surface.³² In order to obtain an average value of the surface roughness, this operation was repeated thirty times; the average, mean and standard deviation are reported.

2.4.3. Elasticity measurements—The nanoscale mechanical properties of electrospun collagen membranes and a 2-D control were characterized by quantitative force volume spectroscopy of individual collagen fibers using AFM.³³ Both collagen membranes were cross-linked prior to the elasticity measurements. A silicon cantilever with an aluminum coated silicon tip (BS-15, Budget Sensors, USA) operated in contact mode was used to obtain a topographical image of individual fibers. Once a fiber was located, a defined force was applied to different regions along the fiber surface, using a calibrated tip. Tip calibration was performed using the thermal tune method and produced a nominal spring constant of approximately 0.2096 N/m, consistent with the manufacturers stated values (force constant: 0.2 N/m, range: 0.07 N/m to 0.4 N/m). The AFM microscope was used to measure elastic properties by collecting force curves over multiple points on the sample surface. A single force curve records the force felt by the tip as it approaches and then is drawn away from the sample.³⁴ Generally, it is more informative to collect a number of force curves across the sample surface, known as force volume imaging using the relative trigger mode.^{35–37}

2.4.4. Statistical analysis—The number of independent replications is indicated for each experiment. Where applicable, the data are expressed as the mean \pm a standard deviation. Student's t-tests with * $p<0.1$ and ** $p<0.05$ were shown to be statistically significant.

2.5. Characterization of C4-2B cells on electrospun collagen membranes (EM)

2.5.1. C4-2B cell culture—C4-2B cells were provided by The Center for Translational Cancer Research (University of Delaware, Newark, DE), and were originally derived from mouse osteoblastic prostate cancer bone metastasis. Cell studies were performed in a Multiscreen dot blot apparatus (BIO-RAD Labs, Hercules, CA) and the collagen-coated TCP (Corning, New York, NY) in a 96-well plate format, which served as a 2-D control. C4-2B cells were maintained in a T-culture medium (Invitrogen, Carlsbad, CA) supplemented with a 5% (v/v) fetal calf serum (Invitrogen, Carlsbad, CA), and 1% (v/v) penicillin/streptomycin (Invitrogen, Carlsbad, CA). The cells were passaged at a dilution of 1:8 every 5 days. The cell culture medium was changed every other day.

2.5.2. Seeding of C4-2B on electrospun collagen membranes—Prior to seeding, electrospun membranes were placed in the dot blot apparatus and sealed in place with parafilm. Membranes were pre-treated with 1% (w/v) glycine solution in PBS for 30 min, followed by a PBS wash, and sterilized with 70% (v/v) ethanol for 30 min. Following subsequent wash steps with PBS, the electrospun collagen membranes were sterilized under UV light overnight. Cells were then seeded at a density of 10^5 cells per well. These experiments were performed in triplicate with collagen-coated (15 µg/ml) TCP in a 96-well culture plate format serving as the 2-D control.

2.5.3. Cell attachment and morphology studies—The number and morphology of C4-2B cells grown on the electrospun collagen membranes were estimated by Laser Scanning Confocal Microscopy (LSCM) (Carl Zeiss, LSC-510, Germany) and Phase Contrast Light Microscopy (PCLM) (Olympus ULS2, Center Valley, PA). Images were taken at 6 random locations on the third day after seeding (seeding density 2×10^5 cells/ml). Prior to imaging, the membranes that had been seeded with C4-2B cells were rinsed twice with PBS and stained

with Cyto13 Green (Molecular Probes, Carlsbad, CA) for 30 min. They then were removed from the stain solution, air-dried and placed onto microscope slides with gel-mount medium (Sigma, St. Louis, MO).

2.5.4. Membrane thickness and cell in-growth—Confocal Z-axis imaging was used to measure the thickness of both electrospun substrates using instrument built-in software (Carl Zeiss, LSC-510, Germany).

2.5.5. Growth of C4-2B cells—In order to evaluate growth properties of cells seeded on various substrates, a WST assay from Roche Applied Science (Roche Molecular Biochemicals, Mannheim, Germany) was used to estimate the total number of viable cells on different substrates. This assay is based on the principle that metabolically active cells will react with a water-soluble tetrazolium salt, identified as WST reagent, to produce a soluble formazan dye that absorbs at 450 nm with a reference wavelength of 405 nm. The number of viable cells was estimated by comparing the absorbance value against a standard curve. C4-2B cells were seeded onto the electrospun collagen membranes inside a 96-well dot blot apparatus, at a cell density of 5000 cells per well in a serum supplemented culture medium. On days 1, 3, 6, and 8, the original medium was removed and 100 μ l of fresh medium was added to each well. WST reagent then was added (10 μ l per well), and plates were incubated for 1h at 37°C, 5% (v/v) CO₂. Collagen-coated TCP in a 96-well plate format served as a 2-D control. Subsequently, the entire medium was harvested and transferred into a new 96-well plate for absorbance measurements in a spectrophotometric plate reader (Dynex Technologies, Chantilly, VA). Because of the differences in surface area between the two membranes and collagen-coated TCP, data were normalized to the absorbance reading of the initial seeding density (4 hours post-seeding).

2.5.6. Cell apoptosis assay—In order to evaluate the death rate of cells attached to both electrospun membranes and a 2-D control, cells were treated with apoptosis inducing cancer drugs CAM (Sigma Aldrich, St. Louis, MO) and DOC (LKT Laboratories, Inc, St. Paul, MN).

A Cell Death Detection Elisa PLUS kit (Roche Applied Science, Palo Alto, CA) was used to analyze the extent of drug-induced cell death. The characteristic feature of apoptosis is DNA fragmentation. The assay is based on a quantitative sandwich-enzyme-immunoassay principle using mouse monoclonal antibodies directed against DNA and histones, respectively. Mono- and oligonucleosomes are present in the cytoplasm of apoptotic cells because DNA degradation occurs several hours before the decomposition of plasma membranes.³⁸ This assay allows specific colorimetric determination of mono-and oligonucleosomes (histone associated DNA fragments) in cell lysates. On the first day after seeding on the electrospun membranes at a density of 10⁵ per well, C4-2B cells were treated with CAM or DOC to induce apoptosis and incubated overnight at 37°C, 5% (v/v) CO₂. The following day, treated cells were lysed, and aliquots (20 μ l) of each sample were placed into a streptavidin-coated microplate. Samples were incubated with anti-histone-biotin and anti-DNA-peroxidase mixture (80 μ l) for 2h on a rotational shaker at room temperature. During the incubation period, nucleosomes are captured via their histone component by the anti-histone-biotin antibody, while binding to the streptavidin-coated microplate. Simultaneously, anti-DNA-peroxidase binds to the DNA portion of the nucleosomes. After removal of the unbound antibodies, the amount of peroxidase retained in the immunocomplex is photometrically determined with ABTS (2,2-azino-di(3-Ethylbenzthiazolinesulfonate-6) as the substrate. Cells grown on collagen-coated TCP in a 96-well plate format served as a 2-D control.

The addition of the drugs was performed after four hours post-seeding (this provides sufficient time for cells to adhere prior to treatment). Cells were then incubated overnight to ensure an efficient penetration of drugs into 3-D matrices. Such a timeline eliminates factors contributing

to the differences in growth rates on various substrates. On day 0 (four hours post-seeding) the number of cells growing on both 3-Ds and 2-D substrates is presumably equal. Additional contributing factors, such as differences in the surface area, and, consequently, differences in the number of attached cells between 2-D and 3-D, led us to express results as the normalized ratio of dead cells treated with drug and untreated (control). The apoptotic index on non-treated (drug concentration 0 ng/ml) cells on each substrate was set as 1. The increase in the apoptotic rate as a result of a drug treatment (apoptotic index) was expressed as an n-fold increase over non-treated cells. Both drugs are water soluble. Hence, an equal amount of water was added to the cells for the control experiment (non-treated).

2.5.7. Fluorescent labeling for filamentous actin—Electrospun collagen membranes were placed on the bottom of eight-well chamber slides, and cells were seeded at a density of 10^5 cells/well. After three days of culture C4-2B cells were fixed with 4% (w/v) paraformaldehyde for 10 min, and then permeabilized with 0.2% (v/v) Triton X-100 in PBS for 10 min at room temperature. The membranes then were blocked for 45 min with 3% (w/v) BSA. Alexa Fluor® 488 nm phalloidin (Invitrogen) was added to each well at a 1:100 dilution in PBS, and incubated for 40 min at 37°C. After extensive washing in PBS, nuclei stain Draq-5 (Biostatus, Leicestershire, UK) at a 1:1000 dilution in PBS was added and incubated for 10 min at room temperature. Membranes were rinsed three times with PBS and then visualized by confocal microscopy.

3. Results

3.1. Characterization of electrospun collagen membranes

3.1.1. Effect of electrospinning processing parameters on fiber size and morphology—We prepared a variety of electrospun collagen and gelatin membranes that differ in pore size, fiber diameter, and extent of cross-linking (related to porosity and elasticity), and identified the conditions, in terms of electrospinning parameters, for successful attachment and growth of cancer cells (preliminary data are not shown). Two membranes with superior cell attachment properties were selected for this study. The collagen fiber mat M1 (produced from HFIP solution) had fiber diameters that ranged from 800 nm to 2500 nm and averaged around 1656 nm (Figure 2A). It will be identified in this text as a microfibrous membrane. In comparison, collagen fiber mat M2 (produced from TFE solution) contained fibers with diameters of 111–536 nm with an average of 319 nm, and we identify it as a nanofibrous membrane. The surface morphology of the electrospun collagen fibers produced from HFIP and TFE solutions appeared to be relatively smooth with small nanoindentations. The membranes are composed of round cross-section collagen fibers that were found to be randomly oriented, giving rise to interconnected pores approximately 6–100 μm in diameter forming a 3-D matrix. The nanofibrous membrane displayed a more uniform fiber diameter and pore size distribution in contrast with the microfibrous membrane (Fig. 2B,D). The concentration of collagen in solution prior to electrospinning was the same in both cases. Such drastic differences in fiber diameter and distribution are attributed to the effect of a solvent's physical characteristics as well as its interactions with collagen α -chains.³⁹ A representative plot of fiber diameter distribution is shown in Fig. 2B. This figure illustrates that there was a small percentage of large fibers produced from TFE solution (approximately 536 nm or larger in diameter) while the majority of fiber diameters were less than 300 nm. Additionally, M2 was characterized by a unimodal distribution of fiber and pore diameters, while M1 showed a multimodal distribution. The average pore diameter before cross-linking was found to be ~9 μm for M1 and ~6 μm for M2.

3.1.2. Cross-linking—In addition to intrinsic differences in fiber diameter due to the nature of the solvent, the cross-linking process could also contribute to modifications of the fiber size

and morphology. Glutaraldehyde vapor protocol was employed for the cross-linking (Scheme 1). As seen in the FESEM micrographs in Fig. 1C,D, the average fiber diameter and morphology are strongly affected by the cross-linking process. The morphology of the cross-linked fibers appears to be more flat, and both pore size and fiber diameter have changed significantly. The FESEM micrographs (Fig. 1B,D) illustrate the changes in fiber morphology that result from cross-linking. The micrographs of the two fibrous meshes were taken in the dry state. In fact, hydration (after incubation in a culture media) also alters fiber morphology (data not shown). The porosity and overall void volume within either electrospun mesh were sufficiently large to allow growth and infiltration of cells inside the scaffold. Further increase in the degree of cross-linking impedes the cells' ability to penetrate inside the fibrous mesh, hence, inhibiting cells' ability to grow inside the electrospun scaffold. These data, as part of preliminary optimization work, are not included.

3.1.3. Surface roughness and topography—Surface roughness of the electrospun collagen fibers is a physical parameter that can be controlled during electrospinning by altering concentration, molecular weight and solvent. Other electrospinning parameters such as applied voltage and flow rate also can alter surface roughness. The collagen fiber topography was assessed by AFM. All images were obtained at 0.459 Hz, scanning 512 lines per image. Collagen cast film deposited on a mica surface served as a control.

The roughness parameter, R_q , calculated as an arithmetic average of the standard deviation of height from central horizontal plane, or root-mean-squared of average height of the surface, was found to influence adhesion properties, such as receptor binding, for adherent cells.³⁰ In this work we intended to evaluate whether this parameter is critical for a non-adherent, anchorage-independent cell line such as C4-2B. The roughness parameter R_q was calculated using AFM software. Surface roughness of the electrospun scaffolds was 30.6 nm and 26.8 nm for M1 and M2 respectively, whereas for collagen film it was 1.4 nm (Fig. 3E).

3.1.4. Substrate stiffness and elastic modulus—To compare the elastic properties of the two fiber membranes with the 2-D control (collagen coated glass slide), force-volume curves were generated at 50 different positions using the relative trigger mode. Each force curve was triggered to produce the same maximum cantilever displacement of 23 nm. Table 2 lists results from the elastic modulus measurements (collagen fibers were crosslinked prior to testing), and Fig. 4 illustrates typical force volume maps and relative elasticity analysis for both electrospun membranes. Elastic moduli for M1 and M2 were found to be around 7.45 MPa and 7.48 MPa respectively. We did not observe any significant changes in the pliability-elasticity of the scaffolds after exposure to ethanol. Previous research performed by our group revealed absence of any significant changes in fiber morphology after ethanol exposure.²⁹ Additionally, exposure to ethanol improves wettability of the original material that is beneficial for scaffold permeability and cellular infiltration.

The membrane's physical properties were also affected by cross-linking. Though the fixed materials are more rigid and stiff than original as-spun fibers, cross-linking does not negate or compromise the pliability of the material with respect to its application as a matrix material for culturing cells. Hydration, which has an impact on fiber morphology and scaffold porosity, can drastically affect the properties of the post-fixed fibers. In the hydrated state, electrospun fibers are not fixed in place, but are rather in a dynamic state of motion. We observed that the pliability of electrospun scaffolds is not compromised, as cells grew inside them by pushing through the fibrous mesh (Fig. 7, 8). Viscoelastic behavior of the hydrated fibers was not investigated in this work, but these efforts are currently underway.

Since the collagen-coated TSP control represents collagen in its monomeric form, tropocollagen, with triple helices of 1.5 nm in diameter, it is quite problematic to accurately

measure the elastic modulus of the 2-D control due to its very small thickness. This limitation can not be addressed using AFM force spectroscopy. However, the elastic moduli of other physiologically relevant materials and TCP are listed in Table 2.

3.2. Characterization of C4-2B cells on electrospun collagen scaffolds

3.2.1. Cell morphology, attachment and spreading—The morphology of C4-2B cells grown on both membranes was visualized by both confocal and light microscopy. Results of these studies (Fig. 5, 6) revealed that cells readily adhered and started to proliferate equally well on both micro- and nanofibrous membranes after three days in a culture medium. Most of the C4-2B cells grown on M1 and M2 were round in shape, and exhibited spheroid-like clustering typical of a native tumor. In contrast, cells grown on 2-D collagen-coated TCP tended to spread out, and had a flat, pancake-like morphology with distorted elongated nuclei.

We also performed light and confocal microscopic imaging to provide morphological evidence of cell spreading, by staining with fluorescently-labeled phalloidin to detect formation and organization of cortical actin. C4-2B cells do not form stress fibers but rather reorganize their cytoskeleton in 3-D. The formation of actin was observed on the periphery of cells in 3-D, while in 2-D it spread out and looked like stress fibers. As shown in Fig. 6, actin formation was observed on both electrospun substrates. However, staining was particularly intense on M1, indicative of active cell spreading on this membrane (Fig. 6D). This morphological feature is typical for highly invasive phenotypes in-vivo. Additionally, in order to provide quantitative assessment of cell spreading we performed a proliferation assay (section 3.2.3).

3.2.2. Substrate thicknesses and cell in-growth—As was previously indicated, cells attached and spread on both electrospun membranes. Substrate thickness is another important parameter (besides porosity) that may relate to the permeability and transport properties of electrospun scaffolds. The membrane thickness is governed by collagen concentration, solvent type, and total volume of the polymer solution; pore size usually correlates to fiber diameter. C4-2B cells infiltrated both membranes on the first day after seeding, with a greater number of cells growing on M2 (Fig. 7). As can be seen from the confocal images, cells grown on M1 migrated farther away from the surface (Fig. 7B).

Results shown in Fig. 8 indicate that increased membrane thickness (~80 µm versus 45µm) does not inhibit the metastatic potential of C4-2B cells, but may enhance tumor cell morphogenesis with an increase in size and number of clusters (compare Fig. 8B to Fig. 7A). Importantly, Fig. 7 and 8 also illustrate that clusters of cells migrated through electrospun membranes of various thicknesses over three and five day periods. Hence, a tumor-specific phenotype, related to a high invasiveness of metastatic prostate cancer cells, was maintained.

3.2.3. Evaluation of cell growth—The growth properties and percentage of cells attached to electrospun fibrous membranes after 1, 3, 6 and 8 days of seeding was assessed by a proliferation (WST) assay. Results (Fig. 9) indicate that on the first day of seeding, the number of cells growing on both membranes and the 2-D control is similar, while on the third and sixth days the number of cells growing on 2-D is slightly higher than on both electrospun membranes. We attribute this time delay to the 3-D architecture with increased thickness and surface area. Some period of time after plating is necessary for cells to migrate inside the matrix and attach to it, after which they start to proliferate. On the eighth day postseeding, a significant increase in the number of C4-2B cells growing on both electrospun membranes relative to the 2-D control was observed. In fact, the number of cells attached to the 2-D control began to decline during the post-confluence phase due to contact-dependant growth inhibition.

Results of statistical analysis indicate that the increased number of viable cells growing on M2 on days 3 and 6 is statistically significant ($p<0.05$), and that the number of cells on M2 is less

than in the 2-D culture (Fig. 9). In contrast, the increase in number of cells growing on M1 (days 3 and 6) is not statistically significant, and is the same as on the 2-D control ($p<0.1$). However, there are no statistically significant differences between the two electrospun membranes and the 2-D control on day 8 (the same number of cells on both membranes and 2-D). Thus, the difference between M1 and M2 is marginal, and can be attributed to the similarity of roughness and elasticity parameters of both membranes. Differences in the observed growth patterns on M1 and M2 (days 3 and 6) may be due to the differences in the specific geometry of each membrane, such as larger pore size (M1), which allow cells to create clusters of greater size.

3.2.4. Apoptosis and drug sensitivity assays—In order to evaluate the susceptibility of C4-2B cells to anti-neoplastic therapeutics, cells were seeded at a high density (10^5 cells/ml) on both electrospun membranes and on a 2-D control. Cells then were incubated with CAM (2 ng/ml) and DOC (170 ng/ml) overnight at 37°C. Untreated cells (NT: no treatment) served as a negative control. After incubation with different drug regimens, aliquots (20 μ l) of cell lysates were analyzed by ELISA. Results of the cell apoptosis assay were calculated using an apoptotic index (specific number of mono- and oligonucleosomes released into the cytoplasm) that is derived from a normalized ratio of the absorbance measurements of drug treated versus non-treated cells (Fig. 10).

The apoptotic index shows the amount of DNA fragments released into the cytoplasm due to apoptosis induced by the drug. Results of the apoptosis assay with CAM are shown in Fig. 10A. The apoptotic index was 1.4 for M1, 2.7 for M2, and 3.0 for 2-D control. These results indicate that survival rate of the cells growing on M1 is almost 2 times higher than on M2 and 2.1 times higher than that of the cells growing on collagen-coated TCP, the 2-D control. Results of the apoptosis assay with DOC are shown on Fig. 10B. In this case, the apoptotic indices were 1.7 for M1, 1.4 for M2, and 2.3 for 2-D control. Results of the statistical analysis with p-value for M1 < 0.05 and for M2 < 0.1 indicate a higher significance level, i.e., drug resistance of C4-2B cells grown on M1 is higher than on M2. Table 3 summarizes our finding and shows the relevance to clinical research. Results are reported for human prostate carcinoma (PC3) and C4-2B cells both *in vivo* and *in vitro*.

4. Discussion

The role that physical parameters play on the suitability of engineered materials for specific biomedical applications is poorly understood. There is a need for a more thorough understanding of the basic material properties that influence cell-specific phenotype. The purpose of this study was not only to evaluate the ability of C4-2B cells to adhere and proliferate on two types of electrospun membranes, but also to correlate biological properties of C4-2B cells with the intrinsic physical characteristics of micro-and nanofibrous collagen scaffolds produced by electrospinning.

As previously reported, the concentration of collagen solutions, flow rate, electrospinning voltage, collection distance and type of solvent all have pronounced effects on fiber diameter and morphology.³⁹ Among them, solvent type and polymer concentration are the most critical parameters influencing 3-D scaffold properties. Previously, we optimized electrospinning parameters to produce continuous fibers without beads and prepared a number of electrospun collagen membranes from a variety of solvents and concentrations. We also performed a feasibility study of cell attachment on various substrates. Based on these data, we selected two membranes that showed good cell attachment properties: M1 and M2. These two electrospun membranes were shown to be different in fiber size and morphology. FESEM micrographs of electrospun porous structures shown in Fig. 1A,C revealed that micron and submicron size fibers were created by electrospinning. The size and morphology of the fibers were observed

NIH-PA Author Manuscript NIH-PA Author Manuscript NIH-PA Author Manuscript

to be greatly influenced by the type of solvent used for electrospinning. For example, HFIP and TFE possess a highly polar OH bond adjacent to a very hydrophobic fluorinated region. Although some controversy exists in the field of research about the effect of HFIP and TFE on collagen molecular structure, we believe that the alcohol portion can hydrogen bond with collagen α -chains, and can also solvate charges on the backbone, thus reducing Columbic repulsion between molecules. Additionally, the hydrophobic portion of these solvents can interact with hydrophobic domains on collagen, countering their tendency to aggregate via hydrophobic interactions. Consequently, α -helices in these solvents are stabilized by stronger intramolecular hydrogen bonds. Thus, the polar nature of these solvents may stabilize a collagen triple-helix; predisposing collagen monomers to undergo polymerization and form helical polypeptides that mimic native collagen fibrils.^{40, 41} Results of some recent studies also suggest that fluorinated alcohols like HFIP and TFE are the best candidates for electrospinning of collagen.⁴²

Interestingly, though collagen fibers electrospun from HFIP solution were almost ten times larger in diameter than fibers electrospun from TFE solution, the results of cell studies indicated that both electrospun collagen membranes are superior 3-D cell culture models for bone adapted prostate cancer cells when compared to a 2-D collagen-coated TCP. This finding differs from the conclusions of recent studies²⁶ suggesting that nanofibers produced by electrospinning must have physical properties closely resembling the 3-D geometry of native ECM in order to be sucessful.^{10, 43} Our results indicate that cells have greater tolerance for variations in fiber size than previously thought.

However, morphological evidence, higher apoptosis resistance, and improved growth properties of C4-2B cells observed on M1 demonstrate the superiority of the microfibrous membrane (M1). Nanofibrous (M2) membranes have limited three-dimensionality,^{44, 45} which can impede cellular infiltration due to a higher density of the mesh resulting from the smaller pore size, reducing mass transport capability.⁴⁶

We speculate that the improved permeability of M1 can be attributed to larger pore sizes: the majority of them range from ~5–100 μm range (in dry state), while the size of C4-2B cells is ~15 μm . However, the distribution is broad with an average of ~9 μm . As we have mentioned earlier, in the hydrated state, pore size increases significantly due to increased plasticity of the fibers allowing them to move freely. The pore sizes are large enough to accommodate cells and their clusters.

Hence, we presume that the membrane geometry, with a micron scale size of the pores, may be adequate for improved diffusion and cellular activity. For example, cell-cell interactions are particularly induced in tumor spheroids found in the 3-D matrix, but not in a 2-D culture, and this is critical for survival and proliferation of C4-2B cells. Considering that the pore sizes of bone marrow loose stromal tissues are in the micron range it is easier to relate membrane-specific geometry to the *in vivo* microenvironment.⁴⁷

Besides fiber geometry, surface topography also acts as an important element governing cell-substrate interactions, including cell adhesion and proliferation. Results of some recent studies demonstrate that cellular behavior is strongly influenced by the nanoscale topography of the substrate.⁴⁸ According to AFM analysis of the samples, the roughness of the electrospun membranes was approximately 30.2 nm for M1 and 26.1 nm for M2, both values higher than that found for a solvent cast collagen film (~1.4 nm) that can be considered a smooth surface. The correlation between cell adhesion and substrate roughness has been studied extensively.⁴⁹ The results of some recent studies suggest that the increased roughness of the polymer surface may contribute to an increased smooth muscle cell adhesion.⁵⁰ Our data does not support these findings, at least in the case of bone adapted prostate cancer cells. Though the

observed difference in surface roughness between two membranes and collagen-coated TCP control is statistically significant, the pattern of cell attachment and growth appeared to be random on both electrospun membranes and the 2-D control. This conclusion, drawn from roughness data, indicates that adhesion properties of C4-2B cells are not influenced by surface topography of the substrate. We hypothesize that for anchorage-independent cancer cell lines, such as C4-2B, surface roughness plays a less significant role, because these cells do not adhere to the substrate in the same way that normal epithelial cells do. Cell signaling from focal adhesion molecules, such as phosphorylation dependent activation of focal adhesion kinase (FAK), is down regulated in 3-D clusters of breast cancer cells suggesting that it may be independent of surface topography of the matrix.⁵¹

Physical cues such as force applied to a cell membrane or stiffness of the material to which cells adhere, are recognized as important characteristics of biological functions. Mechanical stimuli can be as important as chemical ones in determining cell morphology, growth rates, motility and gene expression.⁵² Hence, scaffold elasticity is a critical parameter in material design of artificial extracellular matrices. Table 2 lists the elastic moduli of electrospun collagen membranes along with elastic moduli for some physiologically relevant materials. The AFM force spectroscopy analysis was performed on 3-D matrices with the intention of relating it to other 3-D materials such as hydrogels, whose moduli are in the kPa range. The elasticity values for M1 and M2 (7.45 MPa and 7.48 MPa respectively) are higher than found for ECM of osteoblasts⁵³ (bone cells) ~0.25–0.4 MPa, or epithelial basement membrane (where cancer cells originate) ~0.5 MPa.⁵⁴ This can be partially attributed to the cross-linking process leading to an increased stiffness. The measurements were performed on dry electrospun membranes. We assume that in the hydrated state, which is relevant to their application, these values will be significantly lower, though we did not perform elasticity measurements on the hydrated materials. In contrast, the elastic modulus of TCP that served as a 2-D control is 2.5 GPa⁵⁵ which is three to four orders of magnitude higher than that found in the electrospun fibers and other physiologically relevant substrates listed in Table 2. Such a dramatic difference in elasticity might be partially responsible for the differences in biological properties of C4-2B cells grown in 2-D and 3-D environments.

The compliance of the extracellular matrix differs between tissues and it is altered in tumors. The mechanical properties of scaffolds at the nanoscale level profoundly affect cellular signaling and gene expression related to apoptosis and drug resistance through activation of specific receptors, which sense nanomechanical properties of the engineered ECM. Results of a recent publication showed that the elastic modulus of the ECM has a dramatic effect on mammary epithelial cell morphogenesis that correlates with changes in actin organization and apoptosis resistance.⁵⁶

Both electrospun collagen membranes had higher elastic moduli relative to the hydrogels (commonly used as a substrate for 3-D cultures), though it is significantly lower than TCP, suggesting that increased membrane stiffness, provides an important physical cue, mimicking, to some extent, the physiological environment of bone ECM. These findings support evidence from the literature that cells respond to the mechanical properties of the surrounding matrix material.⁵⁷ Rigid matrices are shown to be especially compatible with tumor cells.^{58–60} *In vivo* studies suggest that women with dense fibrous breast tissue have three to five times higher risk of developing breast cancer.⁵⁸ *In vitro*, breast epithelial cells differentiate into polarized duct-like tubules when cultured in a floating (soft) three-dimensional collagen gel. This differentiation does not occur when the cells are cultured in the same 3-D collagen matrix that is attached to the culture dish, making it more rigid, thus, leading to tumorigenesis.^{59, 60}

One of the major drawbacks of engineered ECMS is their poor permeability due to small pore sizes and high meshwork density. Indeed, an increased membrane thickness may substantially

NIH-PA Author Manuscript NIH-PA Author Manuscript NIH-PA Author Manuscript

modify scaffold density, and consequently permeability, as more fibers overlay on top of each other. Mass transport limitations, toxic metabolic waste build up, lack of nutrients and hypoxic conditions that may exist at greater depths, causes proliferating cells to be mostly found at or near the surface of the solid tumors.⁵⁷ Hence, an increased membrane thickness may contribute to these conditions, and we investigated this parameter as well. The migration of C4-2B cells through the membrane of increased thickness, M1 (~80 μ m) did not show any signs of growth inhibition or morphological changes (Fig. 8) as compared to a thinner membrane (~45 μ m, Fig. 7E). Microfiber scaffolds, in contrast to nanofiber scaffolds, consist of a more spacious, coarser geometry, with fiber diameters up to 10 μ m and corresponding pore sizes of up to 45 μ m.⁶¹ Thus, it may provide a more favorable substrate for infiltration of colony-forming cancer cells, promoting an *in vivo-like* metastatic phenotype in terms of tumor morphogenesis (formation of spheroids), and migratory behavior related to the high invasiveness of C4-2B cells.⁶²

Morphological evidence, such as cell shape, is very important in early detection of the metastatic disease, and is highly influenced by the tumor microenvironment that determines phenotype, gene expression, and finally, survival or apoptosis.⁶³ In this regard, the prostate cancer cells grown on electrospun collagen membranes maintained *in vivo-like* cancer-specific morphology (Fig. 5, Panel II: N and O) including a round shape and a tendency to form three-dimensional tumor spheroids.^{11,12} In contrast, morphological appearance of C4-2B cells growing in 2-D is drastically different: cells adopt flat, pancake-like shape and tend to spread out over the collagen-coated TSP surface (Fig. 5, Panel II: M). The morphology of this surface without cells is shown on Figure 5A.

Active cell spreading and proliferation was also observed in 3-D cultures. Expression of cortical actin, a biochemical marker for cell adhesion and spreading, was particularly strong on M1 (Fig. 6D). Results of a cell proliferation assay with almost linear growth in 3-D suggest that electrospun collagen membranes support the highly-invasive metastatic phenotype of C4-2B cells. In contrast, the proliferation rate in 2-D was inhibited (Fig. 9, day 8), and we attribute this to contact-dependant growth inhibition. In a confluent monolayer culture, cells leave their replicative cycle and reach the quiescent state (G0) or G1/G0 phase of the cell cycle. Many tumor cell lines are subject to contact-dependant growth inhibition in 2-D, and it largely depends on the degree of intercellular adhesion.⁶⁴ The differences between 2-D and 3-D cultures are seen in the shape of the growth curve: almost linear continuous increase in the number of cells growing on M1, while there was some lag in growth observed on M2, versus a plateau shaped curve for 2-D that is typical for a monolayer culture.

Hence, both electrospun collagen membranes support growth and proliferation of C4-2B cells. These data lead to some important conclusions supporting our initial research goal: 1) bone adapted prostate cancer cells can be grown at high confluence on both electrospun membranes over an extended period of time without any visual signs of apoptosis when assessed with vital dye; 2) the highly porous lattice-like architecture of both electrospun substrates allows encapsulation of cells for drug testing without compromising the accuracy of the results due to a significant loss of non-adherent cells during handling (change of media, addition of the drugs, washes, i.e.) that is a common problem in conventional 2-D culture. This is an important advantage of the described 3-D model: cells for drug screening studies must be grown in a highly confluent culture forming spheroids; a condition which occurs naturally in solid tumors *in vivo*.

Systemic chemotherapy with anti-neoplastic agents is a vital part of cancer treatment for breast and prostate cancer, especially after failure of hormone-based interventions.²¹ Because of a greater understanding of important ECM components, receptors and signaling pathways in the tumor microenvironment that operate predominantly in 3-D, new anti-cancer therapeutics are being developed. On the basis of two recent phase III clinical trials, DOC plus prednisone on

a 3 week regimen is now considered standard first-line therapy for metastatic hormone-refractory prostate cancer disease.²¹ Randomized phase III clinical trials are examining DOC in combination with imatinib mesylate (Gleevec), calcitriol and DOC/prednisone in combination with bevacizumab, and an antisense clusterin compound.²¹ Chemotherapy also plays a major role in treatment of breast cancer with a similar interest in combination therapy.^{1,6}

Three-dimensional *in vitro* cell culture systems provide a better approximation of tumor microenvironment, thus providing more accurate responses to drug treatments. For example, mouse mammary tumor cells demonstrate a greater drug resistance to melphalan and 5-fluorouracil as multicellular aggregates than in a 2-D culture.⁶⁵ MDA-MB-231 spheroids exhibit a much lower EC₅₀ to cisplatin when plated in monolayer cultures, than as suspended 3-D spheroids. Treatment of MDA-MB-231 spheroids, but not MDA-MB-231 monolayers, by cisplatin demonstrated that expression of TGF-β1 mRNA and protein was upregulated in a very similar fashion to the drug response patterns of tumor cells *in vivo*.⁶⁶

Our findings support these data. The intrinsic properties of electrospun collagen membranes profoundly affect cellular signaling related to apoptosis. Results of apoptosis assays (Fig. 10) under various drug treatments are summarized in Table 3 where we compared our data with some published results. C4-2B cells were derived from bone marrow primary tumors in mice. They represent the best cell line model to study metastatic prostate cancer. However, most of the clinical trials were performed on commercially available human prostate carcinoma cells PC3. This is the main challenge of the current work. C4-2B cells have not been studied before, either in a 3-D environment or in clinical research. Thus, direct comparison using published results of *in vitro* 2-D studies or clinical trials that utilized PC3 cells in their work is problematic. As for *in vivo* comparisons, we want to emphasize that drug concentrations used *in vivo* are much higher than in 2-D (mg/kg versus ng/ml). Though the direct comparison of drug efficacy *in vivo* and *in vitro* can not be made, our data show good correlation with results of clinical trials.⁶¹ For example, outcomes of some trials revealed high potency of CAM for treatment of metastatic prostate cancer.⁶¹ Results shown in Table 3 (*in vivo* mouse model) indicate a ~83 fold increased efficacy of CAM over DOC.⁶⁰ Our findings show an 85 fold increased efficacy of CAM over DOC using a novel 3-D cancer cell culture system. This presumptive conclusion is made based on the similarity of the apoptotic indices for DOC (1.7) and CAM (1.4) for M1. M1 was chosen because the significance level ($p < 0.05$) is greater than for M2 ($p < 0.1$). Thus, if apoptotic indices are similar for two drugs tested on the same membrane we can draw some assumptions about drug efficacy and it is consistent with the results of clinical trials (Table 3). However, this conclusion is very preliminary and additional testing is needed.

The apoptosis and Live/Dead assay (data not shown) revealed greater drug resistance of C4-2B cells, grown on 3-D electrospun collagen membranes, when compared to a monolayer culture. Interestingly, even though we used a DOC concentration that is significantly higher than in some recently published results,⁶ there is still a dramatic difference in the apoptosis rate between 2-D and 3-D cultures.

Prostate cancer cells in native tumors are anchorage-independent and grow in three-dimensional spheroid-like clusters, where receptor-mediated FAK activation is down regulated.⁵¹ This may well explain why anchorage-independent C4-2B cells growing in clusters on 3-D electrospun collagen matrices are relatively insensitive to microtubule disruption even at high drug concentration. Additionally, resistance to CAM in a 3-D cell culture was lower than found for DOC. The most likely explanation for this finding is differences in drug targeting mechanisms: DOC affects cytoskeleton and microtubules, while CAM targets DNA replication, which should be less dependent on matrix-related spatial

orientation of the cells. This is also in agreement with published results of the clinical trials demonstrating very high antitumor activity of CAM in various cell lines.^{67–69}

Drug diffusion and penetration into 3-D cluster spheroids is another important aspect with respect to drug delivery. Indeed, the penetration of drugs is inhibited in solid tumors. This is one of the reasons why drugs are less efficient *in vivo* than in 2-D *in vitro* culture. Thus, even though some limitation in drug diffusion may exist in the presented 3-D *in vitro* culture model, this does not compromise the overall research goals but rather, closely mimics conditions that exist *in vivo*.

Results of cell studies indicate that electrospun collagen membranes provide a more favorable substrate for cell attachment (Fig. 5), spreading (Fig. 6), migration (Fig. 7, 8), proliferation (Fig. 9), and survival under various drug treatments (Fig. 10) than found for a monolayer or 2-D culture. The highly invasive metastatic phenotype of C4-2B cells was maintained in 3-D cultures.

Another important research objective was to design and characterize a novel 3-D culture system where drug resistance might be higher than in conventional monolayer culture. We accomplished this by determining a minimal effective concentration (lowest drug concentration that induced noticeable differences in apoptosis rates between 2-D and 3-D cultures), and performed concentration testing as part of preliminary work not shown in this manuscript.

This model may aid in finding the lowest effective dose for each cancer patient, and represents a next step toward personalized medicine. The future research will involve culturing of human primary prostate cancer cells on electrospun collagen membranes for *ex-vivo* testing. This approach will allow more accurate (because of the use of human cells) selection of various compounds *in vitro*, optimization of their use, dosing regimens, and determination of specificity and toxicity providing an important means of speeding time to clinical trials, and helping to minimize systemic toxicity, the most devastating side effect of chemotherapy.

Finally, in this work we demonstrated the feasibility of an engineered 3-D cancer cell culture model for drug screening applications *in vitro*. We did not perform *in vivo* studies at this time to compare drug responses; and the described 3-D system should be considered a “concept” rather than a “prototype” model, but after some additional development it can provide a novel and timely tool to test the usefulness of drugs targeting different pathways affecting cancer cell growth.

5. Conclusions

Few studies have considered which substrate material properties influence cell growth while maintaining cell-specific phenotype. In this work we correlated physical properties of electrospun collagen membranes with their biological performance in order to gain some insights into the development of 3-D cancer cell culture models. The importance of physical cues seems to be more pronounced than chemical characteristics. Some recent evidence supports this idea, suggesting that signal transduction in 3-D differs from 2-D, and is highly dependant on the physical state of the substrate.⁷⁰ Therefore, the optimal electrospun scaffold structure is not generic and should be tailored to the specific cell type. Despite the attractive properties of nanofibers for cell attachment, the data presented here strongly encourage the use of microfibrous scaffolds.

In conclusion, there are three important inferences to be made: 1) 3-D *in vitro* cell culture models, based on electrospun collagen fibers, have been shown to reproduce the drug sensitivity pattern of tumor cells *in vivo*, as cancer cells growing on both electrospun

membranes exhibit greater drug resistance compared to a conventional 2-D monolayer culture; 2) electrospun scaffolds provide a new means of allowing the comparison of efficacies of drugs targeting different signaling pathways, and also optimizing dosing regimens; 3) a microfibrous membrane is a better choice of artificial ECM for C4-2B cell culture, providing cell-cell and cell-matrix interactions that are more typical of those found in a native metastatic tumor environment, such as an osteoblastic prostate cancer lesion growing in bone. This structure is the foundation for the development of a controlled and reproducible cell culture model for applications in cancer research and regenerative medicine.^{71, 72}

Supplementary Material

Refer to Web version on PubMed Central for supplementary material.

Acknowledgments

The authors thank Kirk Czymmek for his advice and expertise with laser scanning confocal microscopy. This work was supported by NASA grant "Genetically Engineered Polymers" (NAG8-01923) and NIH, "Cataractogenesis" (NIH 4R33EB803288-03). The project was also supported by NIH grant under INBRE Program of the National Center for Research Resources (NCRR) and NIH/NCI PO1 CA098912.

References

1. Banerjee S, Hussain M, Wang Z, Saliganan A, Che M, Bonfil D, Cher M, Sarkar FH. Cancer Research 2007;67(8):3818–26. [PubMed: 17440096]
2. Helary C, Foucault-Bertaud A, Godeaub G, Coulombe B, Giraud-Guillea MM. Biomaterials 2005;26:1533–1535. [PubMed: 15522755]
3. Ehrman RL, Gey GO. J Natl Cancer Inst 1956;16:1375–1383. [PubMed: 13320119]
4. Woerly S, Plant GW, Harvery AR. Biomaterials 1996;17:301. [PubMed: 8745327]
5. Woerly S. Neurosurg Rev 2002;23:59. [PubMed: 10926098]
6. Sandstrom CE, Bender JG, Miller ME, Papoutsakis ET. Biotechnol Bioeng 1996;50:493–504. [PubMed: 18627011]
7. Horner M, Miller ME, Ottino JM, Papoutsakis ET. Biotechnol Prog 1998;14:689–98. [PubMed: 9758657]
8. Wang R, Xua J, Juliette L, Agapito Castilleja A, Love J, Sunga S-Y, Zhau HE, Goodwin TJ, Chung LW. Semin Canc Biol 2005;15:353–64.
9. Venugopal J, Ramakrishna S. Tissue Eng 2005;11:847–53. [PubMed: 15998224]
10. Abrams GA, Goodman SL, Nealey PF, Franco M, Murphy CJ. Cell Tissue Res 2000;299:39–44. [PubMed: 10654068]
11. Kim JB, Stein R, O'Hare MJ. Breast Canc Res Treat 2004;85(3):281–86.
12. Doillon CJ, Gagnon E, Paradis R, Koutsilieris M. Anticancer Res 2004;24(4):2169–77. [PubMed: 15330157]
13. Radisky DC. J Cell Sci 2005;118:4325–26. [PubMed: 16179603]
14. Tanjore H, Kalluri R. Am J Pathol 2006;168(3):715. [PubMed: 16507886]
15. Gilles C, Polette M, Seiki M, Birembaut P, Thompson EW. Lab Invest 1997;76(5):651–60. [PubMed: 9166284]
16. http://en.wikipedia.org/wiki/Reticularconnective_tissue
17. Glinsky GV, Glinsky VV. Cancer Lett 1996;101:43–51. [PubMed: 8625281]
18. Fidler IJ. Eur J Cancer 1975;9:223–27. [PubMed: 4787857]
19. Stoker AW, Streuli CH, Martins-Green M, Bissell MJ. Curr Opin Cell Biol 1990;2:864–74. [PubMed: 2083086]
20. Thalmann GN, Sikes RA, Wu TT, Degeorges A, Chang SM, Ozen M, Pathak S, Chung LW. The Prostate 2000;44:91. [PubMed: 10881018]
21. Ma PX, Zhang R. J Biomed Mater Res 1999;46:60. [PubMed: 10357136]

22. Yang F, Murugan R, Ramakrishna S, Wang X, Ma YX, Wang S. *Biomaterials* 2003;25:1891. [PubMed: 14738853]
23. Xu CY, Inai R, Kotaki M, Ramakrishna S. *Biomaterials* 2004;25:877. [PubMed: 14609676]
24. Li WJ, Laurencin CT, Caterson EJ, Tuan RS, Ko FK. *J Biomed Mater Res* 2002;60:613. [PubMed: 11948520]
25. Hartgerink JD, Beniash E, Stupp SI. *Science* 2001;294:1684. [PubMed: 11721046]
26. Stephens JS, Fahnestock SR, Farmer RS, Kiick KL, Chase BD, Rabolt JF. *Biomacromolecules* 2005;6(3):1405–13. [PubMed: 15877359]
27. Casper CL, Yang W, Farach-Carson MC, Rabolt JF. *Biomacromolecules* 2007;8(4):1116–23. [PubMed: 17326680]
28. http://www.stehlin.org/research/camptothecin_project.asp
29. Kantoff PW. *Oncology* 2005;19(5):631–636. [PubMed: 15945343]
30. Young F, Xu CYM, Kotaki M, Wang S, Ramakrishna S. *J Biomater Sci Polymer Edn* 2004;15(12):1484.
31. Jastrzebska M, Wrzalik R, Kocot A, Zalewska-Rejdak J, Cwalina B. *J Biomater Sci Polymer Edn* 2003;14(2):185–97.
32. Digital Instrument. Command reference manual 2003:381–400.
33. Shaw GA, McDaniel DP, Elliot JT, Tona A, Plant AL. *Mater Res Soc Symp Proc* 2006;898 E0989-L15-02.1
34. Butt H-J, Cappella B, Kappl M. *Surface Science Reports* 2005;59(1):152.
35. Hoh JH, Heinz WF, A-Hassan E. Digital Instruments. 1997Support Note No.240
36. Fan Y, Chen Q, Ayres VM, Baczevski AD, Udupa L, Kumar S. *Inter Journal of Nanomed* 2008;3(1):4–5.
37. Digital Instruments. Command reference manual. 2003Chapter 14.6
38. www.roche-applied-science.com
39. Matthews JA, Wnek GE, Simpson DG, Bowlin GL. *Biomacromolecules* 2002;3:232–238. [PubMed: 11888306]
40. Sparrow JT, Sparrow DA, Fernando G, Culwell AR, Kovar M, Gotto AM. *Biochemistry* 1992;31:1065. [PubMed: 1734956]
41. Thumb W, Graf C, Parslow T, Schneider R, Auer M. *Spectrochim Acta* 1999;55 A:2729.
42. United States Patent #20080038352.
43. Tsiper MV, Yurchenco PD. *J Cell Sci* 2002;115:1005–07. [PubMed: 11870219]
44. Sahoo S, Ouyang H, Goh JCH, Tay TE, Toh SL. *Tissue Engineering* 2006;12:91–99. [PubMed: 16499446]
45. Ma Z, Kotaki M, Inai R, Ramakrishna S. *Tissue Engineering* 2005;11:101–109. [PubMed: 15738665]
46. Pham QP, Sharma U, Mikos AG. *Biomacromolecules* 2006;7:2796. [PubMed: 17025355]
47. Panoskaltsis N, Mantalaris A, Wu DJ. *J Biosci Bioeng* 2005;100(1):28–30. [PubMed: 16233847]
48. Dalby MJ, Childs MO, Riehle HJ, Johnstone HJ, Affrossman S, Curtis AS. *Exp Cell Res* 2002;276:1–3. [PubMed: 11978003]
49. Lampin M, Warocquier-Clerout R, Legris C, Degrange M, Sigot-Luizard MF. *J Biomed Mater Res* 1997;36:99. [PubMed: 9212394]
50. Thapa A, Webster TJ, Haberstroh KM. *J Biomed Mater Res* 2003;67A:1374.
51. Cukierman E, Pankov R, Stevens DR, Yamada KM. *Science* 2001;294(5547):1708–12. [PubMed: 11721053]
52. Janmey PA, Weitz DA. *Trends in Biochem Sci* 2004;29(7):364. [PubMed: 15236744]
53. Engler AJ, Sen S, Sweeney HL, Discher DE. *Cell* 2006;126:677–89. [PubMed: 16923388]
54. Fisher RF, Hayes BP. *Quart J Exp Physiol* 1982;67:213–224.
55. Chen AA, Khetani SR, Lee S, Bhatia SN, Van Vliet KJ. *Biomaterials* 2009;30(6):1113–20. [PubMed: 19046762]
56. Zahir N, Yeung T, Ming W, Janmey PA, Weaver VM. *Eng Med Biol* 2002;1:431.
57. Discher DE, Janmey P, Wang YL. *Science* 2005;310:1139–43. [PubMed: 16293750]

58. Wozniak MA, Desai R, Solski PA, Der CJ, Keely PJ. *J Cell Biol* 2003;163(3):583–595. [PubMed: 14610060]
59. Keely P, Fong A, Zutter M, Santoro M. *J Cell Sci* 1995;108:595–607. [PubMed: 7769004]
60. Parry G, Lee EY, Farson D, Koval M, Bissell M. *J Exp Cell Res* 1985;156:487–99.
61. Balguid A, Mol A, Marion MH, Bank RA, Bouten CV, Baaijens FP. *Tissue Engineering, Part A* 2008;14:1–8. [PubMed: 18333800]
62. Fu Z, Dozmorov IM, Keller ET. *The Prostate* 2002;51(1):10–20. [PubMed: 11920953]
63. Toh Y-C, Ng S, Khong YM, Zhang X, Zhu Y, Kin P-C, Te C-M, Sun W, Yu H. *Nanotoday* 2006;1(3):34–37.
64. Croix BS, Sheehan C, Rak JW, Florenes VA, Slingerland JM, Robert S, Kerbel RS. *J Cell Biol* 1998;142(2):557. [PubMed: 9679152]
65. Miller BE, Miller FR, Heppner GH. *Cancer Res* 1985;45:4200–05. [PubMed: 4028010]
66. Ohmori T, Yang JL, Price JO, Arteaga CL. *Exp Cell Res* 1998;245(2):350–59. [PubMed: 9851876]
67. www.bioimaging.com
68. Rose WC, Marathe PH, Jang GR, Monticello TM, Balasubramanian BN, Long B, Fairchild CR, Wall ME, Wani MC. *Cancer Chemother Pharmacol* 2006;58:73–85. [PubMed: 16228206]
69. De Cesare M, Pratesi G, Perego P, Carenini N, Tinelli S, Merlini L, Penco S, Pizano C, Bucci F, Vesci L, Pace S, Caposaca F, Carminati P, Zunino F. *Cancer Res* 2001;61:7189–95. [PubMed: 11585754]
70. Wang F, Weaver VM, Petersen OW, Larabell CA, Dedhar S, Briand P, Lupu R, Bissell M. *Proc Natl Acad Sci USA* 1998;95:14821–26. [PubMed: 9843973]
71. Datta MW, Hernandez AM, Schlicht MJ, Kahler AJ, De Gueme AM, Dhir R, Shah RB, Farach-Carson MC, Barrett A, Datta S. *Molecular Cancer* 2006;5(9):12. [PubMed: 16563162]
72. Parker SL, Tong T, Bolden S, Wingo PA. *CA Cancer J Clin* 1997;47(68):5. [PubMed: 8996076]

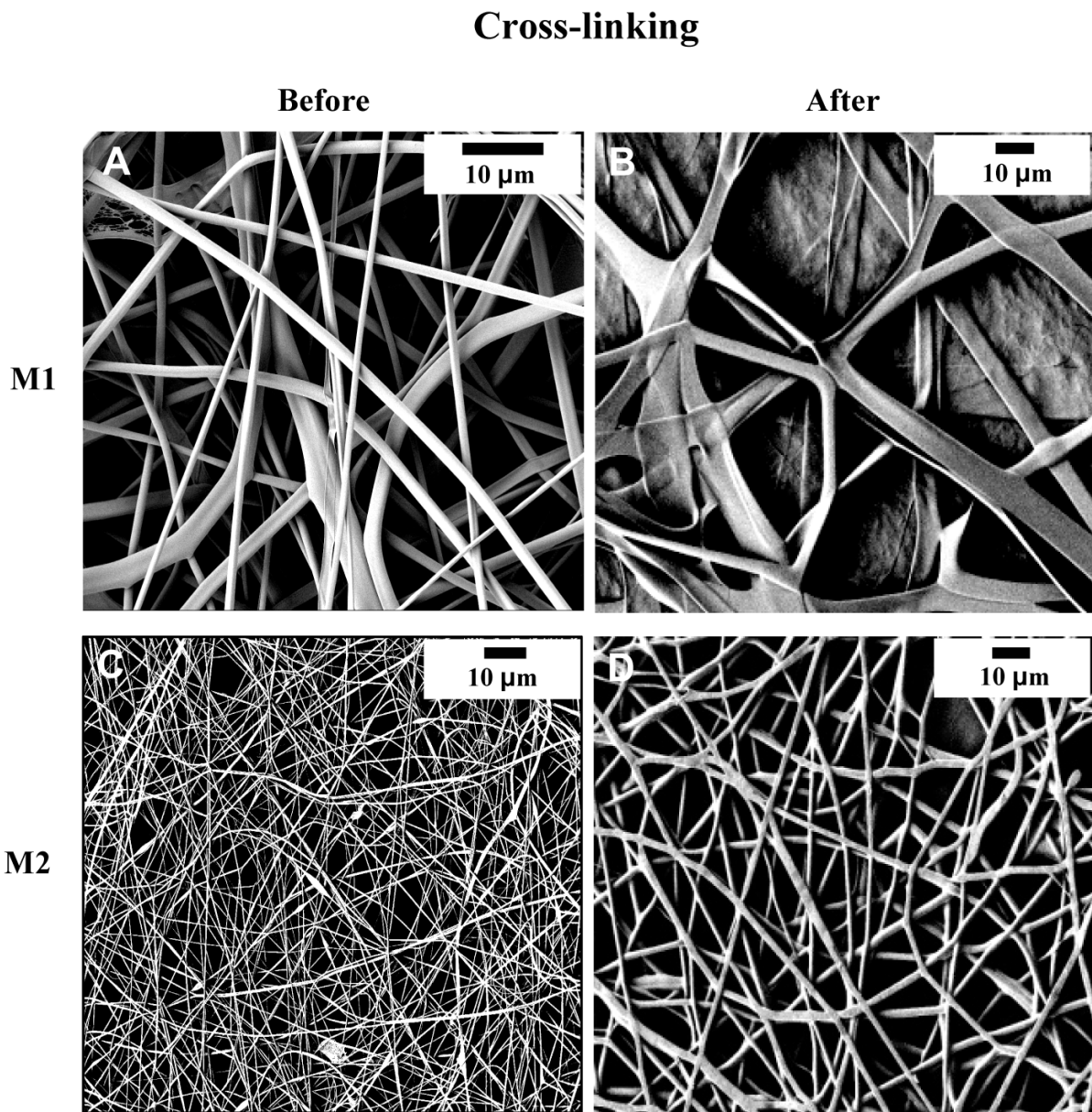
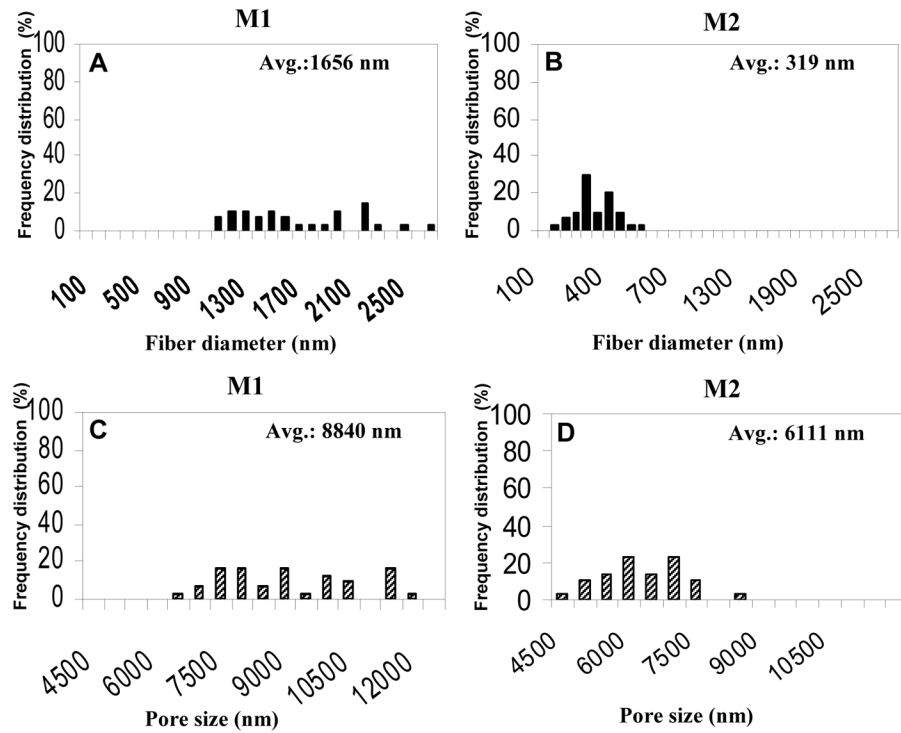
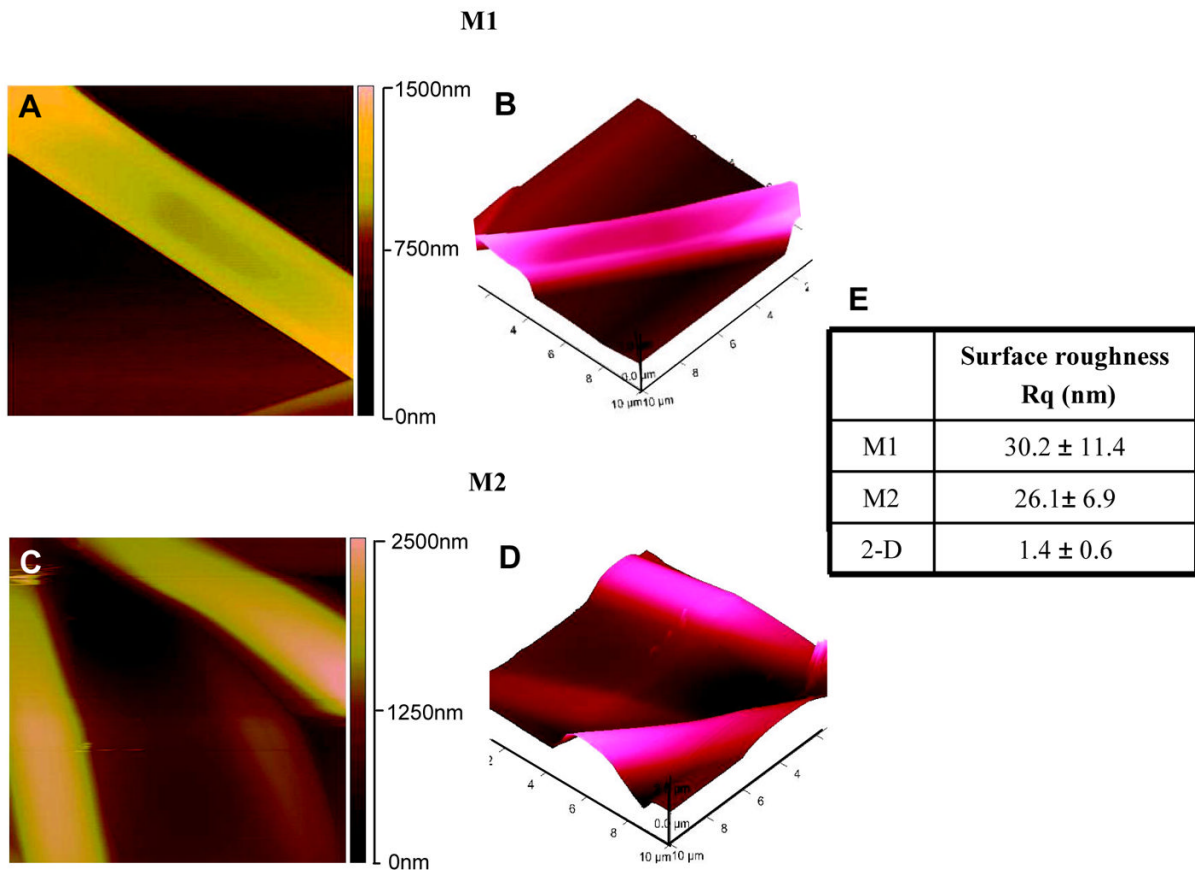


Figure 1.

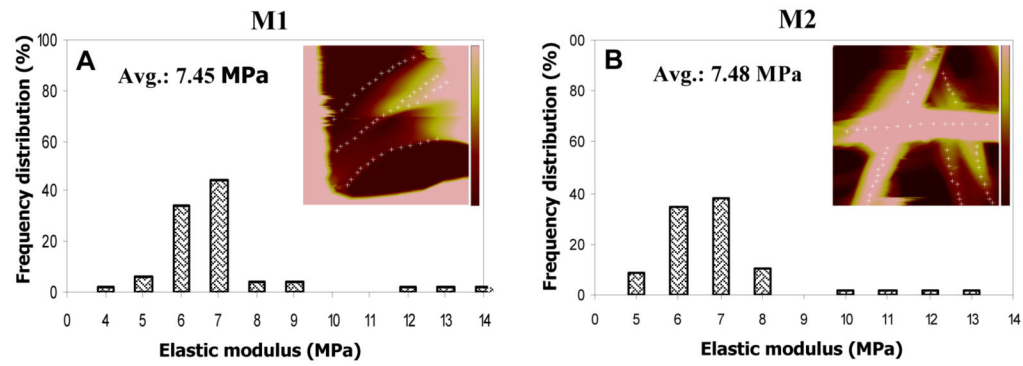
FESEM micrographs of the electrospun collagen membranes: A. M1 (16% (w/v) collagen in HFIP) before cross-linking, B. M1 after cross-linking. C. M2 (16% (w/v) collagen in TFE) before cross-linking, D. M2 after cross-linking. Note that cross-linking causes a significant change in morphology, fiber diameter and pore size.

**Figure 2.**

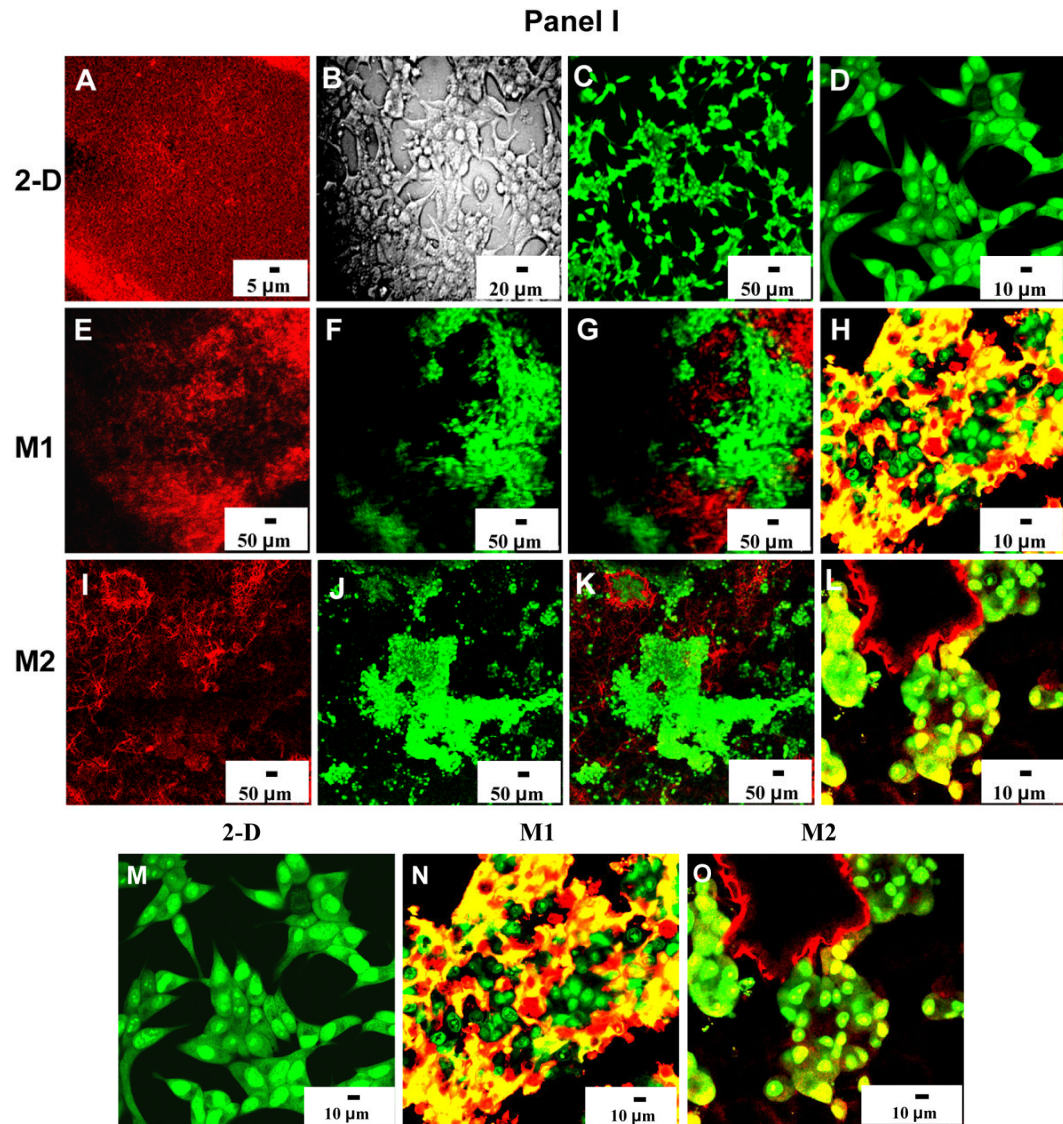
Effect of solvent on fiber diameter and pore size distribution. Fiber diameter: A. M1, n=30. B. M2, n=30. Pore size: C. M1, n=30. D. M2, n=30. All measurements were performed on non-crosslinked dry fibers.

**Figure 3.**

Surface morphology of electrospun collagen membranes: A. Height image of M1 fiber surface. B. 3D surface plot of M1, Z height: 1500 nm. C. Height image of M2 fiber surface. D. 3D surface plot of M2, Z height: 2500 nm. E. Average surface roughness, Rq parameter, measured as root-mean-square of the average height of the surface and reported as mean \pm s.d. Note that 2-D (collagen-coated TCP) has very low Rq , and can be considered a smooth surface. All images were taken using tapping mode, scan size $10 \mu\text{m} \times 10 \mu\text{m}$. Imaging and roughness measurements were performed on non-crosslinked dry fibers.

**Figure 4.**

Relative elasticity of electrospun collagen membranes. A. M1: elastic modulus frequency distribution. Inset shows area map (white marks indicate points where elasticity measurements were taken). B. M2: elastic modulus frequency distribution, inset: area map. Average elasticity: M1~7.45 MPa, M2 ~7.48 MPa. Spring constant 0.2096 N/m, velocity 1.98 μ m/s, and deflection of 151.11nm/V were kept constant using relative trigger mode. Note that both electrospun membranes have very similar relative elasticity profiles with asymmetric “long-tailed” Weibull distribution (shape parameter 2).

**Figure 5.**

Morphology of C4-2B cells grown in 2-D and 3-D cultures (autofluorescence of electrospun collagen fibers shown in red, staining for nuclei is green). **Panel I.** A. LSCM image of collagen-coated TCP (without cells) that served as **2-D** surface. B. Phase Contrast Light Microscopy (PCLM) image of C4-2B cells in **2-D**. C, D. Confocal images of C4-2B cells grown in **2-D**, x10 (C), x40 (D). **M1:** E. Electrospun collagen fibers, single channel image, x10. F. C4-2B cells, single channel image, x10. G. Merged multichannel image of E and F, x10. H. Multichannel image, x40. **M2:** I. Collagen fibers, single channel image, x10. J. C4-2B cells, single channel image, x10. K. Merged multichannel image of I and J, x10. L. Multichannel image, x40. **Panel II.** Morphological differences between 2-D and 3-D cultures observed at higher magnification: **2-D** morphology is characterized by distorted elongated nuclei and flat pancake-like cell shape (M). In contrast, 3-D morphology such as rounding was observed in **3-D:** M1 (N) and M2 (O). Note the differences in type of clustering: cells are tending to spread out on 2-D (M), while in 3-D they grow at high density forming large spheroids (N,O).

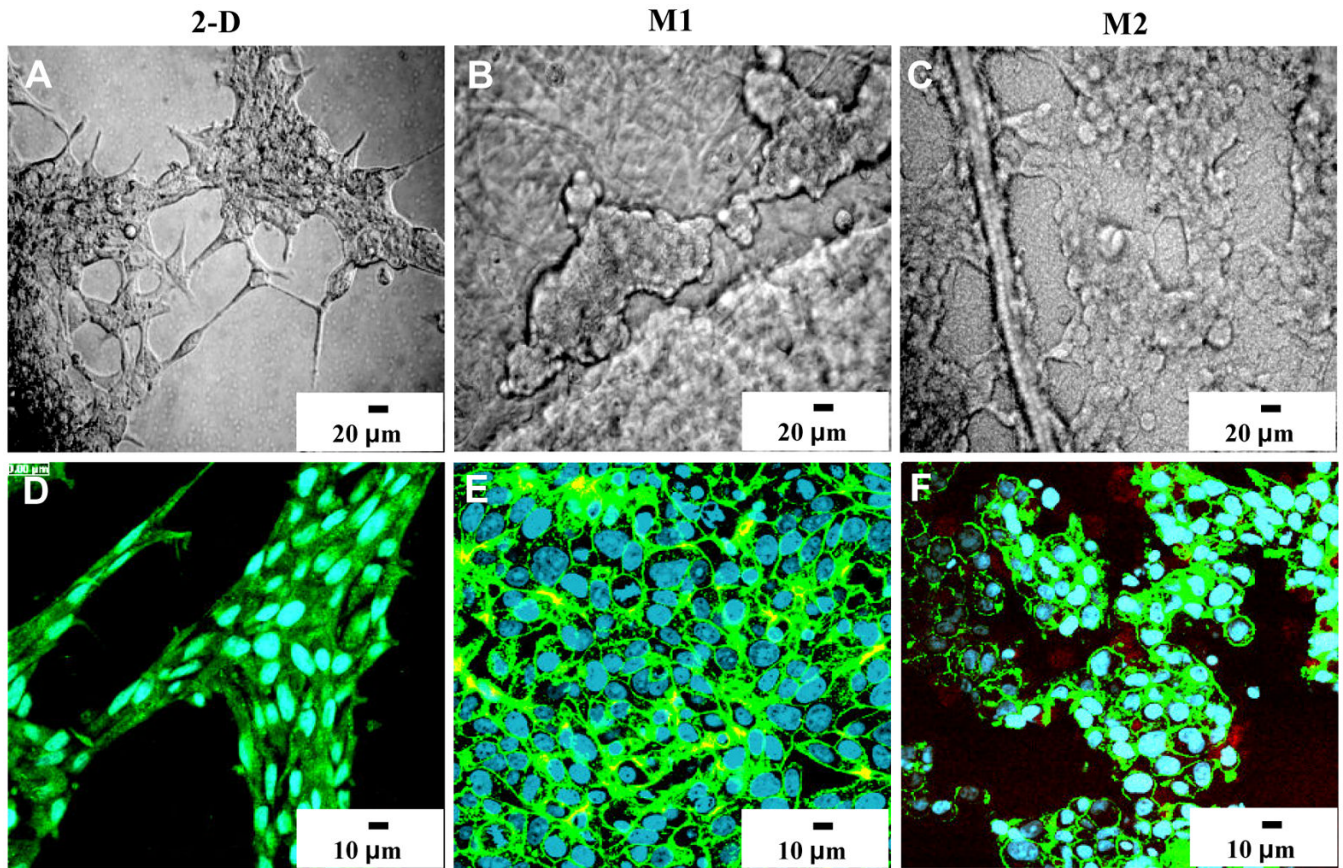
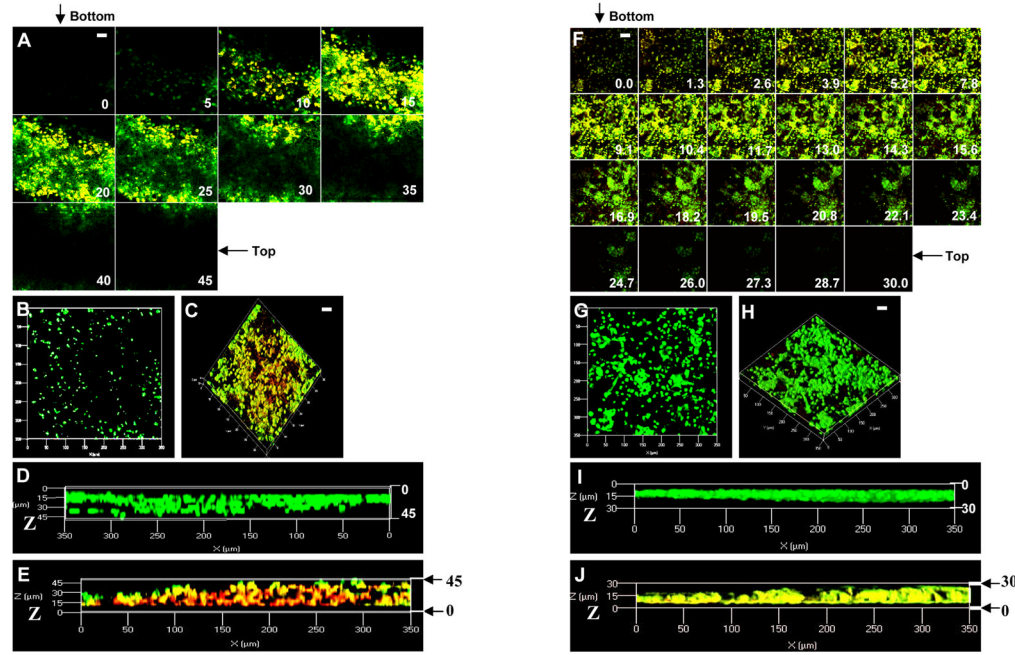
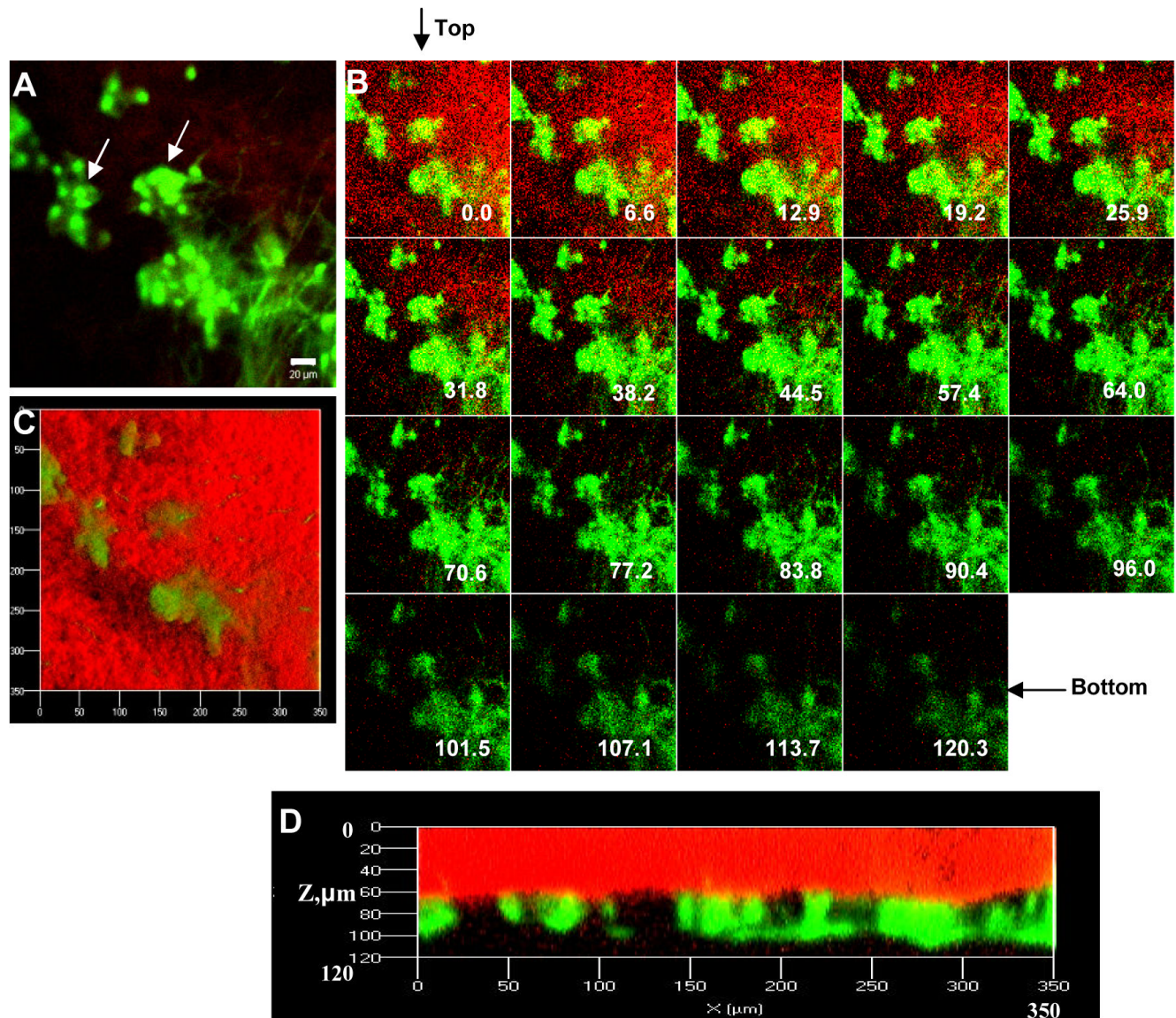


Figure 6.

Reorganization of cytoskeleton in 3-D. PCLM images: A. 2-D. C. M1. E. M2. Confocal images of C4-2B cells stained with nuclear dye Draq-5 (blue). Green staining with Alexa Fluor 488 phalloidin was used to detect changes in cytoskeletal organization: B. 2-D. D. M1. F. M2. Cells grown in 2-D monolayer culture have stretched actin filaments (A, B). C4-2B cells grown on M1 have well defined actin cytoskeleton reflected by robust phalloidin staining at the periphery of cells (D).

**Figure 7.**

In-growth of C4-2B cells on electrospun collagen membranes. Autofluorescence of collagen fibers (red), staining for the nuclei with Cyto 13 (green), scale bar 20 μm . Z-stack images showing C4-2B cells in-growth: A. M1, thickness $\sim 45 \mu\text{m}$. F. M2, thickness $\sim 30 \mu\text{m}$. 3D rendering images reconstructed from z-stacks, top view, single channel showing cells only: B. M1, G. M2. Top view, multiple channels (fibers and cells): C. M1, H. M2. 3D rendering images, side view, single channel: D. M1, I. M2, multiple channels: E. M1, J. M2. Cells infiltrated both 3-D scaffolds on the day 3 post-seeding, though cells grown on M1 have migrated farther away from the surface.

**Figure 8.**

Effect of an increased membrane thickness on metastatic potential of C4-2B cells. Migration of C4-2B cells through M1 over five day time course: A. LSCM image, secondary tumor-like structures (marked by arrows) detached and migrated away from C4-2B spheroids. B. Z-stack of LSCM image. 3D rendering images (reconstructed from Z-stack): C. Top view, area $350 \mu\text{m} \times 350 \mu\text{m}$. D. Side view ("0" on the height scale Z indicates the top of electrospun membrane, thickness $\sim 80 \mu\text{m}$). Red: autofluorescence of collagen fibers, green: staining for the nuclei with Cyto 13, scale bar 20 μm .

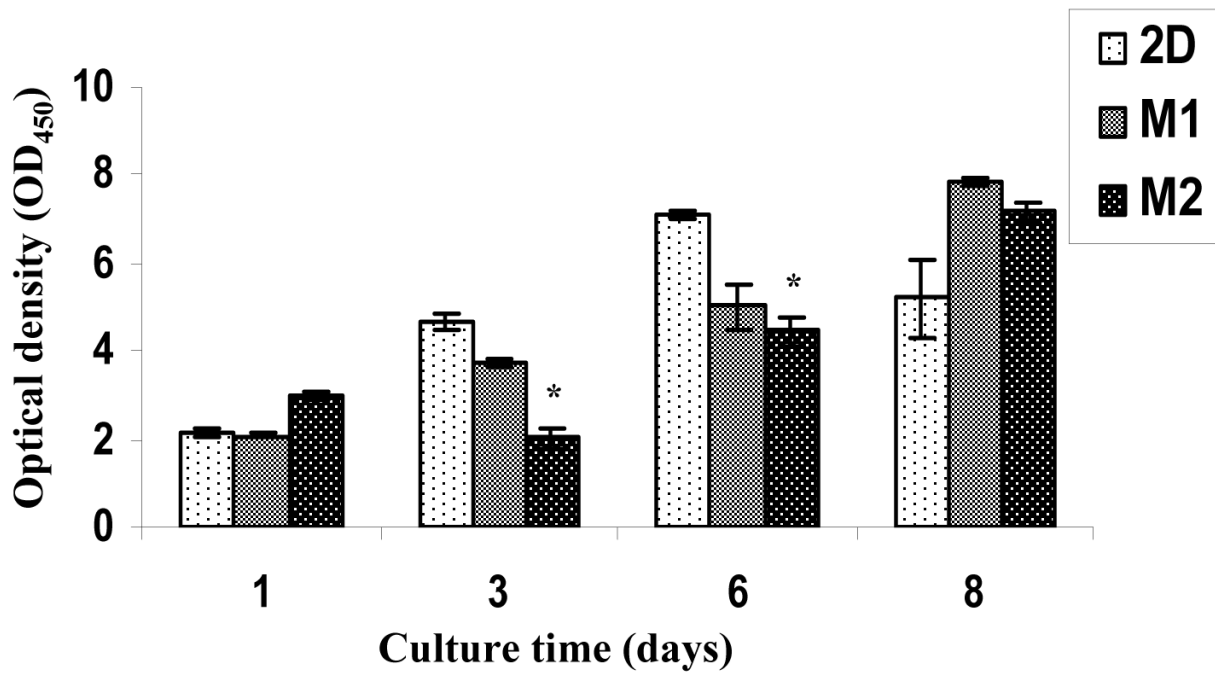
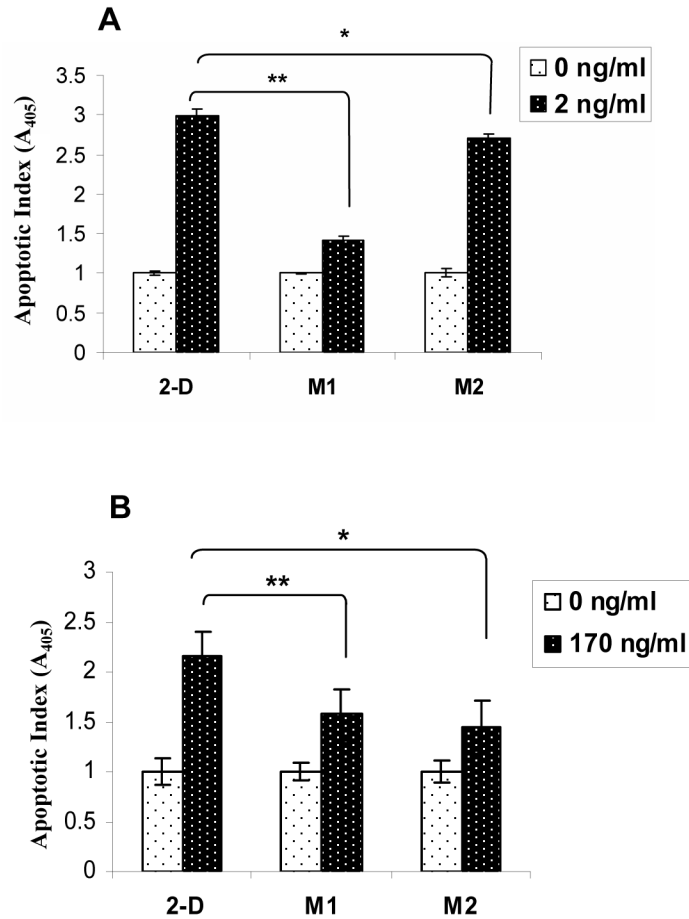
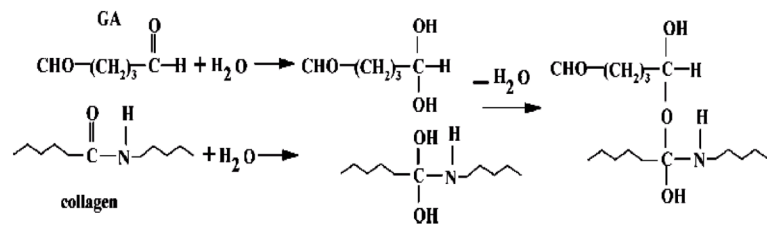


Figure 9.

Proliferation of C4-2B cells over eight day time period (WST assay). Cells grew less at day 3 and day 6 time points in the electrospun collagen membranes compared to 2-D control, and more on day 8 time point. Data are normalized to the absorbance reading of the initial cell density on day 0 after 4 h after seeding, *p<0.05.

**Figure 10.**

DNA fragmentation assay indicating differences in apoptosis rates of C4-2B cells growing on various substrates. A. Cells were treated with camptothecin (CAM) at 2 ng/ml. B. Cells were treated with docetaxel (DOC) at 170 ng/ml. Apoptosis from non-treated cells was set to arbitrary unit of one, and apoptosis from treated cells was normalized to it. * p<0.1, ** P<0.05.



Scheme 1.

Cross-linking reaction of electrospun collagen fibers.

Table 1

Geometry of electrospun collagen membranes. Fiber diameter and pore size of expressed as mean \pm s.d.

Membrane	Fiber diameter (nm)	Pore size (nm)	Thickness (nm)
M1	1542.5 \pm 24.2	8689 \pm 33.5	45
M2	300 \pm 26	6049.5 \pm 41	30

Table 2

Comparison of the elastic moduli found in various physiologically relevant substrates.

Substrate	Elastic Modulus (MPa)
TCP (2-D) 55	2.5×10^3
M1	7.09 \pm 1.8
M2	7.13 \pm 1.6
Electrospun collagen 48	9.4 \pm 2.0
Epithelial BM 72	\sim 0.5
ECM of osteoblasts 51*	0.25-0.40
Type I collagen \sim 50 μ m 49**#	30

Elastic modulus of dried electrospun collagen fibers reported as mean \pm s.d. (n = 50 for M1, n = 47 for M2).

* Note that elastic modulus of hydrated fibers found in ECM of osteoblasts is significantly lower.

** Elastic modulus of collagen fiber bundles \sim 50 μ m in diameter.

Table 3

Apoptosis data analysis.			
Model	CAM	DOC	
<i>In vitro</i> 2-D ^a	0.6 ng/ml [*]	60	0.8 ng/ml ⁵⁹
<i>In vivo</i> (mouse) ^b	0.3 mg/kg [*]	60	0.25 mg/kg ⁵⁹
<i>In vitro</i> 3-D ^c	2 ng/ml	170	ng/ml

* Results are reported for human prostate carcinoma cell line (PC3),

^aEC₅₀ (effective concentration required to induce apoptosis in 50% of cells),

^bMTD (minimal tolerated dose),

^cConcentration tested in this assay was close to EC₅₀.